Design, Synthesis, and Crystal Structure of Hydroxyethyl Secondary Amine-Based Peptidomimetic Inhibitors of Human β-Secretase[†]

Michel C. Maillard,[‡] Roy K. Hom,*,[‡] Timothy E. Benson,*,[§] Joseph B. Moon,[§] Shumeye Mamo,[‡] Michael Bienkowski,[§] Alfredo G. Tomaselli,[§] Danielle D. Woods,[§] D. Bryan Prince,[§] Donna J. Paddock,[§] Thomas L. Emmons,[§] John A. Tucker,[‡] Michael S. Dappen,[‡] Louis Brogley,[‡] Eugene D. Thorsett,[‡] Nancy Jewett,[‡] Sukanto Sinha,[‡] and Varghese John[‡]

Elan Pharmaceuticals, 800 Gateway Boulevard, South San Francisco, California 94080, and Pfizer, Inc., Chesterfield, Missouri 63017 and Ann Arbor, Michigan 48105

Received October 23, 2006

The design and synthesis of a novel series of potent and cell permeable peptidomimetic inhibitors of the human β-secretase (BACE) are described. These inhibitors feature a hydroxyethyl secondary amine isostere and a novel aromatic ring replacement for the C-terminus. The crystal structure of BACE in complex with this hydroxyethyl secondary amine isostere inhibitor is also presented.

Introduction

Alzheimer's disease (AD) is a progressive and ultimately fatal neurodegenerative disorder that afflicts nearly five million people in the United States alone. Intensifying research efforts have focused on understanding the role of AD's neuropathological markers, plaques and tangles, in the disease process.[1] The amyloid cascade hypothesis, which has been the dominant research paradigm, centers around the amyloid β (Aβ) peptide, which is the principal component of the amyloid plaques detected in the brain of AD patients. Although the link between Aβ, either in its partially soluble or aggregated forms, and AD neuronal dysfunction is still controversial, there is, however, compelling biochemical, pathological, and genetic evidence that progressive accumulation of the Aβ peptide within the brain is critically responsible for the neurodegeneration that occurs in AD.[2] Therefore, a strategy aimed at lowering the concentration of neurotoxic Aβ represents an attractive avenue for clinical intervention.[3]

The dominant anti-amyloid (Aβ lowering) approaches that have been pursued are aimed at either increasing Aβ clearance by immunization[4] or decreasing Aβ production or aggregation. The latter approach has focused primarily on two proteolytic enzymes, β- and γ-secretases, that participate in the processing of the amyloid precursor protein (APP).[5] Our discovery program has targeted one of these enzymes, β-secretase, because it plays a crucial role in the first (rate-limiting) step of the amyloid cascade.

In 1999, we along with a number of other laboratories reported on the isolation and cloning of BACE[6−8] (β-site APP-cleaving enzyme) and found that this enzyme has all the functional properties and characteristics of β-secretase. The identification of this promising pharmacological target along with the results from the BACE knockout (BACE -/-) animals, which are normal and devoid of the ability to generate Aβ, has created new hope for the development of effective AD therapeutics.[9] As a first step toward the identification of an orally bioavailable, CNS-active BACE inhibitor, we report herein the rational design of a new series of potent and cell permeable inhibitors of BACE. Compound **6b** represents an advanced BACE inhibitor incorporating the hydroxyethyl secondary amine (HEA) isostere and a nonpeptidic C-terminus. Furthermore, we have determined the X-ray structure of a representative of this series of inhibitors complexed with BACE at a resolution of 1.7 Å.

Inhibitor Design and Results

We have previously reported on the development of potent statine and hydroxyethylene (HE) transition state isostere (TSI)-based inhibitors of BACE using the substrate-based approach.[10] However, these compounds (such as **1**) demonstrated unfavorable cell-to-enzyme (C/E) potency ratios (C/E ∼ 100), which prevented further development of these series. In the search for an alternate TSI compatible with favorable pharmacokinetics, we became interested in the HEA isostere because of its success in the HIV protease (HIV-PR) field.[11] We targeted the hydroxyethyl secondary amine TSI due to the strict preference of BACE for acyclic residues at the S_1' subsite,[12] in contrast to HIV-PR.[13] This TSI, first exploited in the renin field,[14] was especially attractive considering that the majority of CNS drugs contain a basic amine.[15] Furthermore, structural data obtained for acyclic HEA-based inhibitors complexed to HIV-PR revealed a compact network of hydrogen bonds with the catalytic dyad.[16]

The data gathered from our previous studies, using potent HE inhibitors of BACE, provided the basis for our current exploration. The conversion of the HE inhibitor **1** into the HEA inhibitors **2** and **3a** can be envisioned by an insertion of a secondary nitrogen between the methylene and the P_1' substituent in the hydroxyethylene TSI. We found that the preferred configuration for the central Ψ (CH−OH) functionality was opposite to the stereochemistry of other BACE TSIs that we have previously described.[1] For HEA inhibitors of BACE, the (R) configuration of the alcohol afforded the most active inhibitor **3a**, while the (S) isomer **2** was 1000-fold less active (Figure 1). These results are in agreement with that of HEA-based inhibitors of this size in HIV protease[17] and BACE.[18]
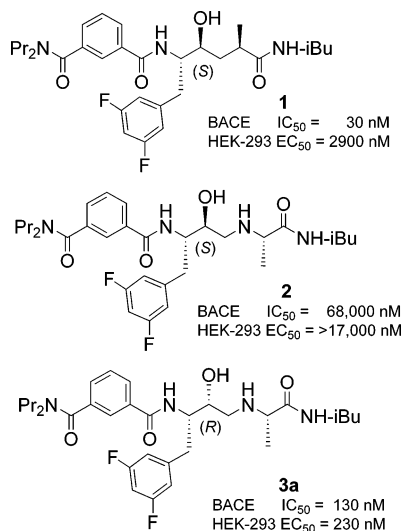
The cellular activity of compound **3a** reinforced our initial hopes for this series. The basic nitrogen did, in fact, appear to favorably impart cellular potency, as similarly observed in another amino-containing BACE inhibitor series.[19] Compound **3a** demonstrated a C/E = 1, while the corresponding neutral

Figure 1. Stereochemistry effects on activity of HEA BACE inhibitors **2** and **3a** as compared with that of HE **1**.

Table 1. Structure of BACE Inhibitors and Enzyme and Cell Activity

cmpd	R_1	R_2	R_3	IC_{50}[a] (nM)	EC_{50}[b] (nM)
3a	H	Me	H	130	230
3b	H	H	Me	500	600
3c	Me	Me	H	70	80
3d	Me	Me	Me	200	230

[a] BACE enzymatic inhibition was determined using MBPC125Swe assay.[8] [b] Cellular inhibition was determined in HEK-293 cells.[28]

hydroxyethylene **1** afforded a C/E = 100. The net effect was a much more potent cellular inhibitor of Aβ production than had been observed in the statine and the HE classes of BACE inhibitors with comparable enzyme potency.

To address the effect of nitrogen insertion on the P_1' SAR, the diastereomeric D-Ala analog **3b** was prepared. This compound exhibited less than 4-fold loss in enzyme inhibitory activity compared to **3a** (Table 1). While studying the P_1' SAR, we continued improving the N-terminal isophthalate and found that methylation of the 3-position of the aromatic ring (**3c**) resulted in a slight improvement of activity. In this new N-terminal variant, dimethylation of the P_1' methylene resulted in only a 3-fold decrease of activity (**3d**).

This relatively flat P_1' SAR suggested that the C-terminal amide may no longer be optimal, which could be attributed to the mainframe shift caused by the nitrogen insertion in the peptidic backbone. We, therefore, became interested in exploring the possibility of replacing the peptidic C-terminus to lower the number of amide bonds and, thus, further enhance the pharmacological profile of this series. We performed a library scan of commercially available primary amines and discovered that the C-terminal amide could be replaced with a benzyl amine. The resulting inhibitor **6a** exhibited submicromolar BACE enzyme activity, which corresponds to only a slight attenuation (2-fold) from amino acid HEA **3c** (Table 2). In addition, compound **6a** demonstrated a cell-to-enzyme ratio (C/E) of 0.3, an improvement from that found in the amino acid HEA

Table 2. Structure of BACE Inhibitors and Enzyme and Cell Activity

cmpd	R_1	IC_{50}[a] (nM)	EC_{50}[b] (nM)
6a	H	130	40
6b	I	5	3
6c	OMe	20	15

[a] BACE enzymatic inhibition was determined using MBPC125Swe assay.[8] [b] Cellular inhibition was determined in HEK-293 cells.[28]

**Scheme 1.** Synthesis of HEA Analogs **3c** and **6b**
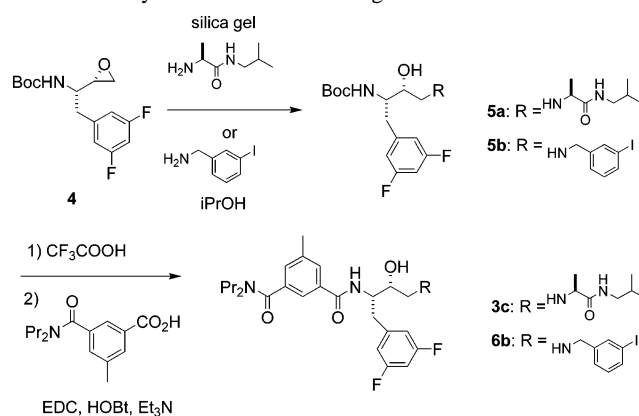
compounds **3c**, suggesting that **6b** may concentrate in the intracellular compartments where BACE is located.

With the discovery of the nonpeptidic C-terminal benzyl amine, a set of benzylamines were selected to prepare a follow-up library. The most potent compound was the *meta*-iodo analog **6b**, which was 25-fold more potent than the parent analog **6a**. A close analog, **6c**, with a *meta*-OMe substituent was also very potent and more drug-like. Thus, **6b** and **6c** were enzymatically more active than the initial lead HE BACE inhibitor **1**, and reduction in the number of amide bonds and introduction of a basic amine into the molecule gave rise to dramatically enhanced cell potency.

Chemistry

The synthesis of compounds **3c** and **6b** was accomplished with a well-known three-step procedure (Scheme 1) starting from the requisite erythro α-amino epoxide **4**, which was prepared according to literature procedures.[20] Epoxide opening in the presence of silica gel[21] or alumina[17,22] afforded the Boc-protected amino alcohol **5a**, which was then deprotected under acidic conditions and underwent amide coupling to provide **3c**. The sequence to form the benzyl HEA **6b** was similar, with the only difference being the epoxide opening, which could be accomplished by heating excess amine in the presence of epoxide **4** in isopropanol. Other HEA analogs **2**, **3b−d**, and **6a,c** were prepared according to the same three-step procedure using the appropriate epoxides,[20,23] N- and C-terminus precursors.

Binding Mode of HEA Inhibitor to BACE. Crystallization of human BACE in the presence of **6b** afforded the opportunity to use X-ray crystallography to characterize the binding mode of this compound within the BACE enzyme active site. Compound **6b** sits at the active site between the catalytic
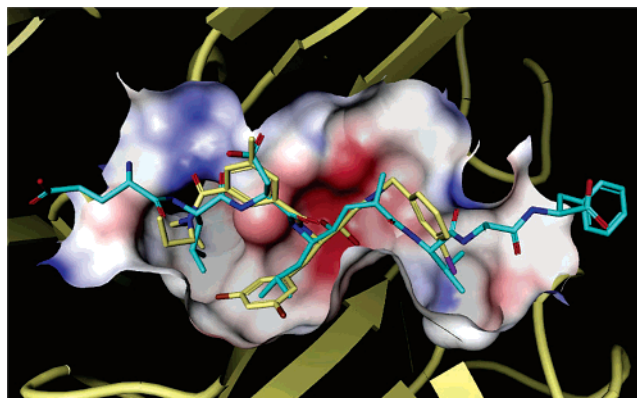
Figure 2. X-ray crystal structure of compound **6b** cocrystallized with human BACE (inhibitor shown with yellow carbon atoms and yellow protein backbone) overlaid with the HE inhibitor OM00-3.[24] The molecular surface shown is derived from the BACE cocrystal structure with **6b** and is colored by electrostatic potential (red, negatively charged; blue, positively charged).
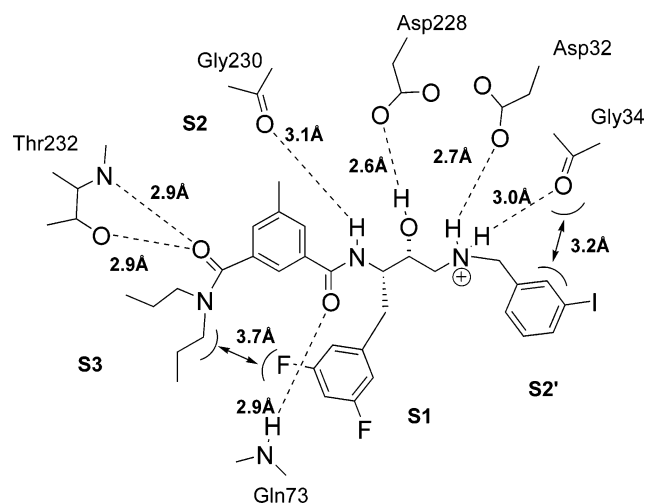
Figure 3. Interactions between compound **6b** and human BACE. Hydrogen bonds are shown with dotted lines. Close interactions detailed in the text are shown with double arrows. Measured distances are indicated along the dashed lines.

aspartates (residues 32 and 228) and the flap (residues 66–76). The inhibitor makes seven key hydrogen bonds with the protein. Interatomic distances consistent with two hydrogen bonds are observed between the N-terminal amide carbonyl oxygen of **6b** and the Thr 232 main chain nitrogen and its side chain hydroxyl (both distances 2.9 Å). Distances and orientations of the flap main chain nitrogen indicate that one hydrogen bond exists between the second amide carbonyl oxygen of **6b** and the Gln 73 main chain nitrogen (2.9 Å). Another hydrogen bond exists between the second amide nitrogen and the main chain carbonyl oxygen of Gly 230 (interatomic distance of 3.1 Å).

As noted above, the erythro configuration of the hydroxy-ethylamine TSI is preferred. The overlay of the crystal structures of BACE in complex with inhibitor **OM00-3**[24] reveals the differences between the HE and HEA insert binding modes to the catalytic aspartates (Figures 2 and 3). The nitrogen insertion in **6b** caused a shift in the position of the isostere hydroxyl group away from its common central position in **OM00-3** between the aspartate residues.[25,26] In contrast to other aspartyl protease inhibitors that mimic the tightly bound water molecule shared between the two aspartates, this HEA hydroxyl interacts with only one of the aspartate residues—Asp 228 (interatomic distance 2.6 Å). Two additional hydrogen bonds are observed

between the protonated HEA nitrogen and the Asp 32 carboxylate side chain (interatomic distance 2.7 Å) and the Gly 34 main chain carbonyl oxygen (interatomic distance 3.0 Å).

These hydrogen bonding interactions are complemented by four key hydrophobic interactions within various subsites. The N-terminal dipropyl groups of the dipropylamide are locked into a configuration that projects one of the propyl groups into the S_3 subsite. The presence of the second propyl group helps to maintain the amide group out-of-plane with respect to the phenyl plane of the isophthalate. In fact, one hydrogen on the first carbon is within van der Waals contact of one of the fluorines present on the di-fluoro phenylalanine (di-F Phe, 3.7 Å). The amide carbonyl makes a 68° out-of-plane twist with respect to the isophthalate group. This twist diminishes the conjugation of this system, which would be very costly without steric constraint provided by the tertiary amide propyl groups interacting with the S_3 subsite. Aryl esters or ketones would pay 4–5 kcal/mol to achieve the 68° out-of-plane twist observed for the dipropyl amide isophthalate groups. A second set of hydrophobic interactions are made by the isophthalate itself with Thr 230, Gln 73, and Arg 235. The isophthalate moiety of **6b** is sandwiched between Thr230 and Gln73 due in part to the close interaction of the Gln73 side chain.

Hydrophobic interactions in S_1 provide a key component of the affinity of **6b**. This pocket is lined with a number of hydrophobic and aromatic side chains (Leu 30, Gln73, Tyr71, Phe 108, Trp115, and Leu118) that create a pocket specifically designed for a Phe-like group on the inhibitor. Gln 73 packs very closely with the isophthalate group, creating a sandwiching interaction. A fourth hydrophobic interaction occurs in S_2' with the C-terminal *meta*-iodo benzyl group. The *meta*-substitution on the C-terminal aromatic group positions the iodine directly into the center of the S_2' subsite. The C-terminal aromatic group also completes a series of stacking interactions between aromatic groups from the protein (Trp 115, Phe 108, Tyr 71, and Tyr 198) and aromatic groups from the inhibitor (diF Phe and C-terminal benzyl).[27] These interactions might explain the increased activity of **6b** compared to **3c**. Additionally, an usually close contact between the aryl hydrogen of the aromatic group and the main chain carbonyl of Gly 34 (3.2 Å) is observed. This proton is positioned similarly to the C-terminal amide N–H of **OM00-3**.

Conclusion

Inhibitors of BACE have the potential to become efficacious agents for the treatment of Alzheimer's disease. In this article, we reported the development of a new series of hydroxyethyl secondary amine-based BACE inhibitors displaying nanomolar potencies in the enzymatic assay. In the initial series containing a peptidic C-terminus, the most active analog **3c** exhibited a strong preference for the (*R*) stereochemistry at the transition state hydroxyl and an excellent C/E ratio. The analysis of the crystal structures of HEA **6b** revealed that the HEA insert created a new trajectory for the peptidic C-terminus compared to HE analogs, which permitted the replacement of the C-terminus amide bond by a phenyl ring. Optimization of the phenyl ring by reintroduction of a P_2' substituent in the *meta*-position led to inhibitors **6b,c**, low nanomolar inhibitors in both enzymatic and the 293 cell-based assays. Compounds **6b,c** are examples of very potent BACE inhibitors with a nonpeptidic C-terminii that extends into the S_2' subsite. These compounds represent a major step toward our goal of identifying a candidate with the required pharmacological properties for CNS activity.

Experimental Section

Chemistry. All reagents were obtained from Aldrich, and all solvents were obtained from VWR. When anhydrous solvents were necessary, Aldrich Sure-Seal solvents were used without further drying. Reaction progress was monitored with analytical thin-layer chromatography (TLC) plates on 0.25 mm Merck F-254 silica gel glass plates. Visualization was achieved using phosphomolybdic acid (PMA), potassium permanganate, or ninhydrin spray reagents or UV illumination. Flash chromatography was performed on E. Merck silica gel 60 (230–400 mesh). ^{1}H NMR spectra were obtained at 300 MHz, respectively, on a Varian or Bruker spectrometer and are reported in parts per million downfield relative to tetramethylsilane (TMS). Low-resolution mass spectra were obtained with a Hewlett-Packard 1100MSD single quad detector using electron spray ionization. Elemental analyses were obtained at the University of California at Berkeley and at Desert Analytics, Tucson, AZ. Compound **1** was prepared as a standard using the literature procedure.[10] Analog **4** was prepared according to literature procedures[20] starting from the commercially available (*S*)-2-*tert*-butoxycarbonylamino-3-(3,5-difluorophenyl)-propionic acid (Synthetech, Inc., Albany, Oregon).

(1*S*,2*R*)-[1-(3,5-Difluorobenzyl)-2-hydroxy-3-(*S*)-(1-isobutyl-carbamoyl-ethylamino)-propyl]-carbamic Acid *tert*-Butyl Ester (5a). Silica gel (Whatman, 230–400 mesh ASTM, 60 A, 1.0 g) was added to a dichloromethane (5 mL) solution of L-alanine isobutylamine (104 mg, 0.72 mmol) and (1*R*,2*S*)-[2-(3,5-difluo-rophenyl)-1-oxiranylethyl]-carbamic acid *tert*-butyl ester (**4**; 200 mg, 0.67 mmol). The resulting suspension was concentrated under reduced pressure, and after standing at room temperature for 3 days, the mixture was purified by flash chromatography (5–95% MeOH/CH$_2$Cl$_2$) to give a white foam as product (190 mg, 64%): ^{1}H NMR (300 MHz, CDCl$_3$) δ 6.75 (m, 2H), 6.65 (m, 1H), 4.45 (d, 1H), 3.75 (m, 1H), 3.55 (m, 1H), 3.2–2.9 (m, 4H), 2.95–2.60 (m, 3H), 1.75 (m, 1H), 1.2–1.3 (m, 12H), 0.9 (d, 3H); (M + H)$^+$ = 444.2.

(1*S*,2*R*)-[1-(3,5-Difluorobenzyl)-2-hydroxy-3-(3-iodobenzyl-amino)propyl]-carbamic Acid *tert*-Butyl Ester (5b). Compound **5b** was prepared in 70% yield from **4** and 3-iodobenzylamine using the procedure detailed above for **5a**. ^{1}H NMR (300 MHz, CDCl$_3$) δ 7.68 (s, 1H), 7.60 (d, *J* = 8.2 Hz, 1H), 7.25 (s, 2H), 6.75 (dd, *J* = 8.0, 2.3 Hz, 2H), 6.65 (tt, *J* = 9.0, 2.2 Hz, 1H), 3.65 (m, 3H), 3.45 (m, 1H), 2.95 (dd, *J* = 12.0, 5.0 Hz, 2H), 2.7–2.8 (m, 3H), 1.38 (s, 9H); (M + H)$^+$ = 533.1. Anal. (C$_{22}$H$_{27}$F$_2$INO$_3$) C, H, N.

(1*S*,2*R*)-*N*-[1-(3,5-Difluorobenzyl)-2-hydroxy-3-(*S*)-(1-isobu-tylcarbamoyl-ethylamino)-propyl]-*N′*,*N′*-dipropyl-isophthal-amide (2). Compound **2** was prepared according to the same procedure described for compound **3c** starting from the threo epoxide.[20a] ^{1}H NMR (300 MHz, CDCl$_3$) δ 7.7 m (1H), 7.40–7.20 (m, 3H), 6.80 (m, 2H), 6.60 (m, 1H), 4.35 (m, 1H), 3.75 (m, 1H), 3.40 (m, 2H), 3.25 (m, 1H), 3.2–2.95 (m, 6H), 2.75 (m, 2H), 2.55 (m, 1H), 1.70 (m, 4H), 1.50 (m, 2H), 1.30 (m, 4H), 0.95 (m, 3H), 0.85 (m, 7H), 0.7 (m, 3H); (M + H)$^+$ = 575.4. Anal. (C$_{31}$H$_{44}$F$_2$N$_4$O$_4$·TFA·2H$_2$O) C, H, N.

(1*S*,2*S*)-*N*-[1-(3,5-Difluorobenzyl)-2-hydroxy-3-(*S*)-(1-isobu-tylcarbamoyl-ethylamino)-propyl]-*N′*,*N′*-dipropyl-isophthal-amide (3a). Compound **3a** was prepared according to the same procedure described for compound **3c**. ^{1}H NMR (300 MHz, CDCl$_3$) δ 7.70 (m, 1H), 7.4 (m, 1H), 7.1 (m, 2H), 6.8 (m, 2H), 6.65 (m, 1H), 4.35 (m, 1H), 3.70 (m, 1H), 3.45 (m, 2H), 3.10–2.95 (m, 6H), 2.65 (m, 2H), 2.45 (m, 1H), 1.70 (m, 2H), 1.50 (m, 1H), 1.25 (2d, *J* = 7 Hz, 4H), 0.95 (t, 3H), 0.90 (m, 7H), 0.7 (m, 3H); (M + H)$^+$ = 575.6. Anal. (C$_{31}$H$_{44}$F$_2$N$_4$O$_4$·TFA·H$_2$O) C, H, N.

(1*S*,2*R*)-*N*-[1-(3,5-Difluorobenzyl)-2-hydroxy-3-(*R*)-(1-isobu-tylcarbamoyl-ethylamino)-propyl]-*N′*,*N′*-dipropyl-isophthal-amide (3b). Compound **3b** was prepared according to the same procedure described for compound **3c**. ^{1}H NMR (300 MHz, CDCl$_3$) δ 7.80 (m, 1H), 7.7 (m, 1H), 7.3 (m, 2H), 6.8 (m, 2H), 6.58 (m, 1H), 4.30 (m, 1H), 3.70 (m, 1H), 3.40 (m, 2H), 3.10–2.80 (m, 6H), 2.70 (m, 2H), 2.60 (m, 1H), 1.70 (m, 2H), 1.50 (m, 1H), 1.25 (2d, *J* = 7 Hz, 4H), 0.95 (t, 3H), 0.90 (m, 7H), 0.7 (m, 3H); (M + H)$^+$ = 575.4. Anal. (C$_{31}$H$_{44}$F$_2$N$_4$O$_4$·TFA·H$_2$O) C, H, N.

(1*S*,2*R*)-*N*-[1-(3,5-Difluoro-benzyl)-2-hydroxy-3-(*S*)-(1-isobu-tylcarbamoyl-ethylamino)-propyl]-5-methyl-*N′*,*N′*-dipropyliso-phthalamide (3c). Compound **5a** (271 mg, 0.61 mmol) was dissolved in 20 mL of 15% trifluoroacetic acid in dichloromethane at 0 °C. After 3 h, the reaction mixture was concentrated in vacuo. The crude amine salt was used without further purification. The crude amine trifluoroacetate salt was dissolved in dry dichloromethane (20 mL) and cooled to 0 °C. Triethylamine (0.5 mL, 3.5 mmol) and 5-methyl-*N*,*N*-dipropyl-isophthalamic acid (176 mg, 0.67 mmol) were added, followed by hydroxybenzotriazole (HOBt, 165 mg, 1.22 mmol) and 1-(3-dimethylaminopropyl)-3-ethylcar-bodiimide hydrochloride (EDC, 233 mg, 1.22 mmol). This mixture was stirred at 0 °C for 1 h then allowed to warm to room temperature overnight. The mixture was then partitioned between 10% citric acid (10 mL) and EtOAc (10 mL), and the aqueous layer was extracted with EtOAc (3 × 10 mL). The combined organic layers were washed (NaHCO$_3$, NaCl), dried (Na$_2$SO$_4$), filtered, and concentrated under reduced pressure. Flash chromatography gave a white foam as product (282 mg, 79%): R_f = 0.3 (10% MeOH/CH$_2$Cl$_2$); ^{1}H NMR (300 MHz, CDCl$_3$) δ 7.45–7.2 (m, 2H), 7.1 (m, 1H), 6.80 (m, 2H), 6.65 (m, 1H), 4.35 (m, 1H), 3.70 (m, 1H), 3.40 (m, 2H), 3.10–2.95 (m, 7H), 2.65 (m, 2H), 2.5 (m, 1H), 2.32 (m, 3H), 1.70 (m, 4H), 1.45 (m, 2H), 1.25 (2d, 4H), 0.95 (m, 3H), 0.85 (m, 7H), 0.7 (m, 3H); (M + H)$^+$ = 589.3. Anal. (C$_{32}$H$_{46}$F$_2$N$_4$O$_4$·TFA·1.5H$_2$O) C, H, N.

(1*S*,2*R*)-*N*-[1-(3,5-Difluorobenzyl)-2-hydroxy-3-(1-isobutylcar-bamoyl-1-methyl-ethylamino)-propyl]-5-methyl-*N′*,*N′*-dipropyl-isophthalamide (3d). Compound **3d** was prepared according to the same procedure described for compound **3c**. ^{1}H NMR (300 MHz, CDCl$_3$) δ 7.45–7.2 (m, 2H), 7.15 (s, 1H), 6.80 (m, 2H), 6.65 (m, 1H), 4.35 (m, 1H), 3.70 (m, 1H), 3.40 (m, 2H), 3.10–2.80 (m, 7H), 2.60 (m, 2H), 2.5 (m, 1H), 2.30 (m, 3H), 1.70 (m, 4H), 1.45 (m, 2H), 1.30 (m, 4H), 0.95 (m, 3H), 0.85 (m, 7H), 0.7 (m, 3H); (M + H)$^+$ = 603.6. Anal. (C$_{33}$H$_{48}$F$_2$N$_4$O$_4$·TFA·0.5H$_2$O) C, H, N.

(1*S*,2*R*)-*N*-[1-(3,5-Difluorobenzyl)-2-hydroxy-3-(benzylamino)-propyl]-5-methyl-*N′*,*N′*-dipropylisophthalamide (6a). Compound **6a** was prepared from **5b** using the two-step procedure described below for **6c**. The white foam obtained was dissolved in dichloromethane and treated with HCl/Et$_2$O. After stirring overnight, the precipitate was collected by filtration and dried. ^{1}H NMR (CDCl$_3$) δ 7.55–7.40 (m, 5H), 7.33 (s, 2H), 6.80 (dd, *J* = 8.2, 2.3 Hz, 2H), 6.62 (tt, *J* = 9.0, 2.2 Hz, 1H), 4.30–4.10 (m, 3H), 4.00–3.80 (m, 1H), 3.47 (t, *J* = 7.7 Hz, 2H), 3.40–3.20 (m, 1H), 3.20–3.00 (m, 4H), 2.82 (dd, *J* = 14.4, 11.7 Hz, 1H), 2.41 (s, 3H), 1.80–1.60 (m, 2H), 1.60–1.40 (m, 2H), 1.00 (t, *J* = 7.4 Hz, 3H), 0.69 (t, *J* = 7.4 Hz, 3H); (M + H)$^+$ = 552.3. Anal. (C$_{32}$H$_{39}$F$_2$N$_3$O$_3$·2H$_2$O·HCl) C, H, N.

(1*S*,2*R*)-*N*-[1-(3,5-Difluorobenzyl)-2-hydroxy-3-(3-iodobenzyl-amino)-propyl]-5-methyl -*N′*,*N′*-dipropylisophthalamide (6b). Compound **6b** was prepared from **5b** using the two-step procedure described below for **6c**. The white foam obtained was dissolved in dichloromethane and treated with trifluoroacetic acid. After stirring overnight, the precipitate was collected by filtration and dried. ^{1}H NMR (CDCl$_3$) δ 7.80 (s, 1H), 7.75 (d, *J* = 8.2 Hz, 1H), 7.50 (s, 2H), 7.40 (d, *J* = 8.2 Hz, 1H), 7.15 (m, 2H), 6.80 (dd, *J* = 8.2, 2.3 Hz, 2H), 6.60 (tt, *J* = 9.0, 2.2 Hz, 1H), 4.15 (m, 2H), 3.95 (m, 1H), 3.75 (m, 1H), 3.50–3.35 (m, 2H), 3.10 (m, 3H), 2.85–2.60 (m, 3H), 2.32 (s, 3H), 1.70 (m, 2H), 1.45 (m, 2H), 0.98 (t, *J* = 7.0 Hz, 3H), 0.71 (t, *J* = 7.1 Hz, 3H); (M + H)$^+$ = 678.2. Anal. (C$_{32}$H$_{38}$F$_2$IN$_3$O$_2$·TFA) C, H, N.

(1*S*,2*R*)-*N*-[1-(3,5-Difluorobenzyl)-2-hydroxy-3-(3-methoxy-benzylamino)-propyl]-5-methyl-*N′*,*N′*-dipropylisophthalamide (6c). (1*S*,2*R*)-[1-(3,5-Difluorobenzyl)-2-hydroxy-3-(3-methoxybenzyl-amino)-propyl]-carbamic acid *tert*-butyl ester, prepared as compound **5b** (255 mg, 0.59 mmol), was dissolved in 2 mL of 50% trifluoroacetic acid in dichloromethane at rt. After 1 h, the reaction mixture was concentrated in vacuo. The crude amine salt was used without further purification. The crude amine trifluoroacetate salt was dissolved in dry DMF (3 mL) and cooled to 0 °C. Triethylamine (0.5 mL, 3.6 mmol) and 5-methyl-*N*,*N*-dipropyl-isophthalamic acid

(258 mg, 0.59 mmol) were added, followed by hydroxybenzotriazole (HOBt, 157 mg, 1.16 mmol) and 1-(3-dimethylaminopropyl)-3-ethylcarbodiimide hydrochloride (EDC, 230 mg, 1.2 mmol). This mixture was stirred at 0 °C for 5 min then allowed to warm to room temperature overnight. The mixture was then partitioned between 10% citric acid (10 mL) and EtOAc (10 mL), and the aqueous layer was extracted with EtOAc (3 × 10 mL). The combined organic layers were washed (NaHCO$_3$, NaCl), dried (Na$_2$SO$_4$), filtered, and concentrated under reduced pressure. Flash chromatography gave a white foam as product (222 mg, 65%): R_f = 0.3 (10% MeOH/CH$_2$Cl$_2$); ^{1}H NMR (CDCl$_3$) δ 7.45 (s, 1H), 7.34 (s, 1H), 7.30−7.10 (m, 3H), 6.89 (d, J = 7.2 Hz, 2H), 6.85−6.70 (m, 1H), 6.80 (dd, J = 8.2, 2.3 Hz, 2H), 6.62 (tt, J = 9.0, 2.2 Hz, 1H), 4.40−4.25 (m, 1H), 3.90−3.70 (m, 2H), 3.79 (s, 3H), 3.70−3.55 (m, 1H), 3.55−3.35 (m, 2H), 3.20−2.95 (m, 3H), 2.90 (dd, J = 14.2, 8.9 Hz, 1H), 2.82−2.68 (m, 2H), 2.32 (s, 3H), 2.11 (br s, 2H), 1.80−1.58 (m, 2H), 1.58−1.40 (m, 2H), 0.98 (t, J = 7.0 Hz, 3H), 0.71 (t, J = 7.1 Hz, 3H); (M + H)$^+$ = 582.6. Anal. (C$_{33}$H$_{41}$F$_2$N$_3$O$_4$) C, H, N.

BACE Enzyme and Aβ Cell Assays. β-Cleavage ELISA assays were carried out in 200 mM sodium acetate, pH 4.8, 0.06% Triton X-100, with 10 μg/mL MBPAPPC125 (or MBP-C125). MBP-C125 is a fusion protein containing the maltose-binding protein at the amino terminal end connected to the carboxyl-terminal 125 amino acids of APP (amyloid precursor protein) at the carboxyl terminal end. Reaction mixtures were incubated at 37 °C for 1−2 h, and the quenched reaction mixtures were then loaded onto 96-well plates coated with a polyclonal antibody raised to MBP. Generated β-cleaved product was detected using biotinylated Sw192 or biotinyated Wt192 as specific reporter antibodies and quantitated against the appropriate MBP-C125 standard. The 293Swe cell assays were performed according to the protocol previously described.[28]

X-Ray Crystallography. A DNA construct of human BACE was prepared in the *E. coli* pQE70 expression vector missing 35 amino acids of the pro-segment (sequence started at Arg36 and continued to Ser342) and containing a C-terminal His$_6$ tag. Details of the expression, purification, and crystallization will be published in detail elsewhere. In short, the crystallization conditions were as follows: 8 mg/mL purified BACE, 16% PEG 3000, and 0.1 M sodium acetate, pH 4.6. Crystals were grown at 20 °C and grew to approximately 0.6 × 0.15 mm. Before data collection, the crystals were cryoprotected in crystallization buffer plus 30% glycerol and flash frozen in liquid nitrogen crystals of BACE in the presence of **6b** diffracted to 1.7 Å resolution at the Advanced Photon Source (IMCA-CAT beamline 17-ID) with unit cell dimensions of a = 73.1 Å, b = 105.1 Å, c = 50.5 Å, α = γ = 90°, β = 94.8° in space group *C*2 with one molecule per asymmetric unit. The complex of BACE with compound **6b** was refined using CNX to an R-factor of 20.6% and a free-R factor of 23.1%. The coordinates for the structure of the BACE/compound **6b** complex have been deposited in the Protein Data Bank under access code 2IQG.

Note Added after ASAP Publication. There was an error in the numbering of the aspartate residues in the third paragraph of Chemistry in the version published ASAP January 10, 2007; the corrected version was published ASAP January 18, 2007.

Supporting Information Available: Combustion analysis data of final compounds. This material is available free of charge via the Internet at http://pubs.acs.org.

References

(1) Selkoe, D. J. Translating cell biology into therapeutic advances in Alzheimer's disease. *Nature* **1999**, *399* (6738 Suppl), A23−A31.

(2) Jorge, G.; Blas, F. Amyloidosis and Alzheimer's disease. *Adv. Drug Delivery Rev.* **2002**, *54*, 1539−1551.

(3) Citron, M. β-Secretase inhibition for the treatment of Alzheimer's disease—promise and challenge. *Trends Pharmacol. Sci.* **2004**, *25*, 92−97. Citron, M. Strategies for disease modification in Alzheimer's disease. *Nat. Rev.* 2004, *5*, 677−685. Jorge, G.; Blas, F.; Ghosh, A.; Hong L.; Tang J. β-Secretase as a therapeutic target for inhibitor drugs. *Curr. Med. Chem.* **2002**, *9*, 1135−1144.

(4) Schenk, D.; Barbour, R.; Dunn, W.; Gordon, G.; Grajeda, H.; Guido, T.; Hu, K.; Huang, J.; Johnson-Wood, K.; Khan, K.; Kholodenko, D.; Lee, M.; Liao, Z.; Lieberburg, I.; Motter, R.; Mutter, L.; Soriano, F.; Shopp, G.; Vasquez, N.; Vandevert, C.; Walker, S.; Wogulis, M.; Yednock, T.; Games, D.; Seubert, P. *Nature* **1999**, *400*, 173−177.

(5) Esler, W. P.; Wolfe, M. S. A portrait of Alzheimer secretases—New features and familiar faces. *Science* **2001**, *293*, 1449−1454.

(6) Vassar, R.; Bennett, B. D.; Babu-Khan, S.; Kahn, S.; Mendiaz, E. A.; Denis, P.; Teplow, D. B.; Ross, S.; Amarante, P.; Loeloff, R.; Luo, Y.; Fisher, S.; Fuller, J.; Edenson, S.; Lile, J.; Jarosinski, M. A.; Biere, A. L.; Curran, E.; Burgess, T.; Louis, J.-C.; Collins, F.; Treanor, J.; Rogers, G.; Citron, M. β-Secretase cleavage of Alzheimer's amyloid precursor protein by the transmembrane aspartic protease BACE. *Science* **1999**, *286*, 735−741.

(7) Yan, R.; Bienkowski, M. J.; Shuck, M. E.; Miao, H.; Tory, M. C.; Pauley, A. M.; Brashier, J. R.; Stratman, N. C.; Mathews, W. R.; Buhl, A. E.; Carter, D. B.; Tomasselli, A. G.; Parodi, L. A.; Heinrikson, R. L.; Gurney, M. E. Membrane-anchored aspartyl protease with Alzheimer's disease β-secretase activity. *Nature* **1999**, *402*, 533−537.

(8) Sinha, S.; Anderson, J. P.; Barbour, R.; Basi, G. S.; Caccavello, R.; Davis, D.; Doan, M.; Dovey, H. F.; Frigon, N.; Hong, J.; Jacobson-Croak, K.; Jewett, N.; Keim, P.; Knops, J.; Lieberburg, I.; Power, M.; Tan, H.; Tatsuno, J.; Tung, J.; Schenk, D.; Seubert, P.; Suomensaari, S. M.; Wang, S.; Walker, D.; Zhao, J.; McConlogue, L.; John, V. Purification and cloning of amyloid precursor. *Nature* **1999**, *402*, 537−540.

(9) Roberds, S. L.; Anderson, J.; Basi, G.; Bienkowski, M. J.; Branstetter, D. G.; Chen, K. S.; Freedman, S.; Frigon, N. L.; Games, D.; Hu, K.; Johnson-Wood, K.; Kappenman, K. E.; Kawabe, T.; Kola, I.; Kuehn, R.; Lee, M.; Liu, W.; Motter, R.; Nichols, N. F.; Power, M.; Robertson, D. W.; Schenk, D.; Schoor, M.; Shopp, G. M.; Shuck, M. E.; Sihna, S.; Svensson, K. A.; Tatsuno, G.; Tintrup, H.; Wijsman, J.; Wright, S.; McConlogue, L. BACE knockout mice are healthy despite lacking the primary β-secretase activity in the brain: implications for Alzheimer's disease therapeutics. *Hum. Mol. Genet.* **2001**, *10*, 1317−1324.

(10) (a) Hom, R. K.; Gailunas, A. F.; Mamo, S.; Fang, L. Y.; Tung, J. S.; Walker, D. E.; Davis, D.; Thorsett, E. D.; Jewett, N. E.; Moon, J. B.; John, V. Design and synthesis of hydroxyethylene-based peptidomimetic inhibitors of human β-secretase. *J. Med. Chem.* **2004**, *47*, 158−164. (b) Hom, R. K.; Fang, L. Y.; Mamo, S.; Tung, J. S.; Guinn, A. C.; Walker, D. E.; Davis, D. L.; Gailunas, A. F.; Thorsett, E. D.; Sinha, S.; Knops, J. E.; Jewett, N. E.; Anderson, J. P.; John, V. Design and synthesis of statine-based cell-permeable peptidomimetic inhibitors of human β-secretase. *J. Med. Chem.* **2003**, *46*, 1799−1802.

(11) Randolph, J. T.; DeGoey, D. A. Peptidomimetic inhibitors of HIV protease. *Curr. Top. Med. Chem.* **2004**, *4*, 1079−1095. Abdel-Rahman, H.; Al-karamany, G.; El-Koussi, N. HIV protease inhibitors; peptidomimetic drugs and future perspective. *Curr. Med. Chem.* **2002**, *9*, 1905−1922.

(12) Turner, R.; Koelsch, G.; Hong, L.; Castenheira, P.; Ghosh, A.; Tang, J. Subsite specificity of memapsin 2 (β-secretase): Implications for inhibitor design. *Biochemisty* **2001**, *40* (34), 10001−10006.

(13) Roberts, N. A.; Matin, J. A.; Kinchington, D.; Broadhurst, A. V.; Craig, J. C.; Duncan, I. B.; Galpin, S. A.; Handa, B. K.; Kay, J.; Kröhn, A.; Lambert, R. W.; Merrett, J. H.; Mills, J. S.; Parkes, K. E. B.; Redshaw, S.; Ritchie, D. L.; Taylor, D. L.; Thomas, G. J.; Machin, P. J. Rational design of peptide-based HIV proteinase inhibitors. *Science* **1990**, *248*, 358.

(14) (a) Dann, J.; Stammers, D.; Harris, C. J.; Arrowsmith, R.; Davies, D.; Hardy, G.; Morton, J. Human renin: A new class of inhibitors. *Biochem. Biophys. Res. Commun.* **1986**, *134*, 71−77. (b) Ryono, D.; Free, C.; Neubeck, R; Samaniego, S.; Godfrey, J.; Petrillo, E. *Proc. Am. Pept. Symp., 9th* **1985**, 739.

(15) Ajay, B.; Murcko, M. Designing libraries with CNS activity. *J. Med. Chem.* **1999**, *42*, 4942−4951.

(16) (a) March, D. R.; Abbenante, G.; Bergman, D. A.; Brinkworth, R. I.; Wickramasinghe, W.; Begun, J.; Martin, J. L.; Fairlie, D. P. Substrate-based cyclic peptidomimetics of Phe-Ile-Val that inhibit HIV-1 protease using a novel enzyme-binding mode. *J. Am. Chem. Soc.* **1996**, *118*, 3375−3379. (b) Dohnalek, J.; Hasek, J.; Duskova, J.; Petrokova, H.; Hradilek, M.; Soucek, M.; Konvalinka, J.; Brynda, J.; Sedlacek, J.; Fabry, M. Hydroxyethylamine isostere of an HIV-1 protease inhibitor prefers its amine to the hydroxy group in binding to catalytic aspartates. A synchrotron study of HIV-1 protease in complex with a peptidomimetic inhibitor. *J. Med. Chem.* **2002**, *45*, 1432−1438.

(17) Tucker, T. J.; Lumma, W. C., Jr.; Payne, L. S.; Wai, J. M.; De Solms, S. J.; Giuliani, E. A.; Darke, P. L.; Heimbach, J. C.; Zugay, J. A.; Schleif, W. A.; Quintero, J. C.; Emini, E. A.; Huff, J. R.; Anderson, P. A. A series of potent HIV-1 protease inhibitors containing a hydroxyethyl secondary amine transition state isostere: Synthesis, enzyme inhibition, and antiviral activity. *J. Med. Chem.* **1992**, *35*, 2525−2533.

(18) Stachel, S.; Coburn, C.; Steele, T.; Loutzenhiser, E.; Gregro, A.; Rajapakse, H.; Lai, M.-T.; Crouthamel, M.-C.; Xu, M.; Tugusheva, K.; Lineberger, J.; Pietrak, B.; Espeseth, A.; Shi, X.-P.; Chen-Dodson, E.; Holloway, M.; Munshi, S.; Simon, A.; Kuo, L.; Vacca, J. Structure-based design of potent and selective cell-permeable inhibitors of human β-secretase (BACE-1). *J. Med. Chem.* **2004**, *47*, 6447−6450.

(19) Yang, W.; Lu, W.; Lu, Y.; Zhong, M.; Sun, J.; Thomas, A.; Wilkinson, J.; Fucini, R.; Lam, M.; Randal, M.; Shi, X.-P.; Jacobs, J.; McDowell, R.; Gordon, E.; Ballinger, M. Aminoethylenes: A tetrahedral intermediate isostere yielding potent inhibitors of the aspartyl protease BACE-1. *J. Med. Chem.* **2006**, *49*, 839−842.

(20) (a) Rich, D.; Sun, C. Q.; Vara Prasad, J.; Pathiasseril, A.; Toth, M.; Marshall, G.; Clare, M.; Mueller, R.; Houseman, K. Effect of hydroxyl group configuration in hydroxyethylamine dipeptide isosteres on HIV protease inhibition. Evidence for multiple binding modes. *J. Med. Chem.* **1991**, *34*, 1222−1225. (b) Getman, D.; DeCrescenzo, G.; Heintz, R.; Reed, K.; Talley, J.; Bryant, M.; Clare, M.; Houseman, K.; Marr, J.; Mueller, R.; Vazquez, M.; Shieh, H.-S.; Stallings, W.; Stegeman, R. Discovery of a novel class of potent HIV-1 protease inhibitors containing the (*R*)-(hydroxyethyl)urea isostere. *J. Med. Chem.* **1993**, *36*, 288−291. (c) Rotella, D. Stereoselective synthesis of *erythro* α-amino epoxides. *Terahedron Lett.* **1995**, *36*, 5453−5456.

(21) Bennett, F.; Patel, N.; Girijavallabhan, V.; Ganguly, A. The synthesis of novel HIV-protease inhibitors via silica gel assisted addition of amines to epoxides. *Synlett* **1993**, 703−704.

(22) Posner, G.; Rogers, D. Organic reactions at alumina surfaces. Mild and selective opening of arene and related oxides by weak oxygen and nitrogen nucleophiles. *J. Am. Chem. Soc.* **1977**, *99*, 8214−8218.

(23) Luly, J.; Dellaria, J.; Plattner, J.; Soderquist, N. A synthesis of protected aminoalkyl epoxides from α-amino acids. *J. Org. Chem.* **1987**, *52*, 1487−1492.

(24) Hong, L.; Turner, R.; Koelsch, G.; Shin, D.; Ghosh, A. K.; Tang, J. Crystal structure of memapsin 2 (β-secretase) in complex with an inhibitor OM00-3. *Biochemistry* **2002**, *41*, 10963−10967.

(25) Hong, L.; Koelsch, G.; Lin, X.; Wu, S.; Terzyan, S.; Ghosh, A. K.; Zhang, X. C.; Tang, J. Structure of the protease domain of memapsin 2 (β-secretase) complexed with inhibitor. *Science* **2000**, *290* (5489), 150−153.

(26) Rich, D. Pepstatin-derived inhibitors of aspartic proteinases. A close look at an apparent transition-state analog inhibitor. *J. Med. Chem.* **1985**, *28*, 263−273.

(27) Patel, S.; Vuillard, L.; Cleasby, A.; Murray, W.; Yon, J. Apo and inhibitor complex structures of BACE (β-secretase). *J. Mol. Biol.* **2004**, *343*, 407−416.

(28) Dovey, H.; John, V.; Anderson, J.; Chen, L.; de Saint Andrieu, P.; Fang, L.; Freedman, S.; Folmer, B.; Goldbach, E.; Holsztynska, E.; Hu, K.; Johnson-Wood, K.; Kennedy, S.; Kholodenko, D.; Knops, J.; Latimer, L.; Lee, M.; Liao, Z.; Lieberburg, I.; Motte, R.; Mutter, L.; Nietz, J.; Quinn, K. Functional γ-secretase inhibitors reduce β-amyloid peptide levels in brain. *J. Neurochem.* **2001**, *76*, 173−181.